

---

# Combining Different Types of Gravity Observations in Regional Gravity Modeling in Spherical Radial Basis Functions

Katrin Bentel and Michael Schmidt

---

## Abstract

With the increasing number of high-resolution gravity observations, which became available in the recent years, global Earth gravity models can be regionally refined. While global gravity models are usually represented in spherical harmonic basis functions with global support, a very promising option to model the regional refinements is the use of spherical radial basis functions with quasi-compact support. We use the approach of regional gravity modeling in spherical radial basis functions, with parameter estimation to determine the coefficients of the signal representation, on a test data set provided by the IAG-ICCT study group JSG0.3. We demonstrate on the data set for Europe that the approach is well-suited for different types of observations, such as terrestrial, aerial, and satellite-based measurements, as well as their combination. Furthermore, our results contribute to the study group's goal of inter-comparison of different modeling methodologies. Our regional modeling approach leads to relative errors of about 0.2–2% when compared to the validation data sets on the topography.

---

## Keywords

Combination of different observations • ICCT study group test data • Radial basis function • Regional gravity field modeling

---

## 1 Introduction

A study group under the umbrella of the IAG (International Association of Geodesy)—ICCT (Inter Commission Committee on Theory) between Commission 2 (Gravity Field) and Commission 3 (Earth Rotation and Geodynamics) titled as *Joint Study Group JSG0.3 Comparison of Current Methodologies in Regional Gravity Field Modeling* was established in 2011 with duration until 2015. The goal of this study group is to compare different regional

modeling methodologies and to finally outline standards and conventions for future regional gravity products. One of the activities so far was to provide synthetic test data sets which are used for inter-comparison of regional gravity modeling methodologies. Among the objectives are the choice of the type of basis function, the point grid, an appropriate methodology to solve the adjustment problem, and the consideration of errors.

Details on the study group as well as the test data can be found online at <http://jsg03.dgfi.badw.de>. Synthetic gravity observations of different types are provided for two different regions in Europe and in South America. For each region satellite-based, aerial, as well as terrestrial observations are provided, along with noise information for each observations type, and validation data sets in terms of disturbing gravity potential on the topography.

We use the test data sets in Europe for our regional gravity modeling approach in spherical radial basis functions.

---

K. Bentel (✉)

Department of Mathematical Sciences and Technology, Norwegian University of Life Sciences, IMT, Postboks 5003, 1432 Ås, Norway  
e-mail: [katrin.bentel@umb.no](mailto:katrin.bentel@umb.no)

M. Schmidt

Deutsches Geodätisches Forschungsinstitut, Munich, Germany

In Chap. 2 we explain the approach, in Chap. 3 we present our results with the individual data sets, and in Chap. 4 their combination. Finally, in Chap. 5 all modeling results are summarized and discussed. Thereby, with this article, we contribute to the goal of the study group of inter-comparison of different regional gravity modeling approaches by presenting our results with the study group's test data.

## 2 Regional Gravity Modeling in Spherical Radial Basis Functions

For regional gravity modeling, we use spherical radial basis functions, as presented in Freeden et al. (1998), Holschneider et al. (2003), or Schmidt et al. (2007) and references therein, amongst many others. We follow the approach given in Bentel et al. (2013). A regional residual gravity signal  $\Delta F$  is represented in a series expansion in spherical radial basis functions according to

$$\Delta F(\mathbf{x}) = \sum_{k=1}^K d_k B(\mathbf{x}, \mathbf{x}_k). \quad (1)$$

Thereby,  $B(\mathbf{x}, \mathbf{x}_k)$  are the radial basis functions, which depend only on the spherical distance between their location point  $\mathbf{x}_k$  and the evaluation point  $\mathbf{x}$ , and are defined as

$$B(\mathbf{x}, \mathbf{x}_k) = \sum_{n=0}^N \frac{2n+1}{4\pi R^2} \left(\frac{R}{r}\right)^{n+1} B_n P_n(\mathbf{x}, \mathbf{x}_k). \quad (2)$$

$P_n$  are the Legendre polynomials,  $R$  is the radius of a reference sphere (e.g. mean Earth radius), and  $r$  is the radius of the evaluation point  $\mathbf{x}$ . The coefficients  $B_n$  define the type of radial basis function. For the computations here, we use cubic polynomial radial basis functions, motivated by the findings in Bentel et al. (2013). They are defined by

$$B_n = \left(1 - \frac{1}{N}n\right)^2 \left(\frac{2}{N}n + 1\right), \quad (3)$$

and can be found in Freeden et al. (1998). The values for  $N$  are adjusted according to the signal which is to be modeled. With  $\mathbf{x}$ , the different types of observations are directly used at the locations at which they are obtained. The points  $\mathbf{x}_k$ , the locations for the radial basis functions, are chosen on a Reuter grid, see Freeden et al. (1998).

To determine the coefficients  $d_k$  of the regional signal representation, regularization is needed due to the downward continuation problem of gravity which is involved and due to non-uniqueness of the coefficients to be estimated. We use variance component estimation according to Koch and

Kusche (2002) to determine the variance components of the data sets and the prior information. The variance components can further be used to determine relative weighting factors between the different data sets as well as the regularization parameter with respect to the prior information. Prior information in terms of the expectation vector for the coefficients to be estimated is added. We set the vector of prior information equal to zero, because a residual signal is modeled after removing a reference field (EGM 96) up to spherical harmonic degree 60. All results presented here are obtained with sets of physically meaningful coefficients, what means they are correlated to the signal to be modeled as well as small on the margins, which are needed beyond the area of observations in order to avoid boundary effects. They are between  $2^\circ$  and  $3^\circ$  wide.

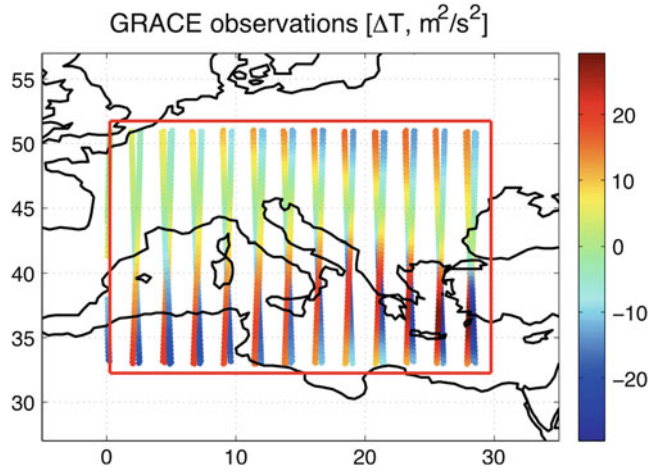
All modeling approaches are validated with the given validation data sets. From the regional gravity field representation, the disturbing potential is synthesized at the same points where validation data is available, respectively in the area where observations are available after subtracting a margin width. This is necessary to avoid boundary value effects and the margin widths are given together with the results in Table 1. Then the errors in terms of differences in each point are computed as well as a relative RMS error value in terms of percentage of the error RMS from the signal RMS of the full signal up to degree 2,190.

## 3 Different Examples of Gravity Observations in Europe

We use the test data provided by the ICCT study group ready for download at <http://jsg03.dgfi.badw.de> with the given realistic level of white noise on the observations. For the test region in Europe, two sets of synthetic observations are provided for each observation type. Satellite-based observations are available from GRACE (Tapley et al. 2004) and GOCE (Drinkwater et al. 2007), two sets of aerial observations are available for two different flight campaigns, and the terrestrial observations are available on a regular grid on the topography with two different grid spacings, one with  $30'$  and the other with  $5'$  spacing. From all different types of observations, a reference field (EGM 96) up to spherical harmonic degree 60 is removed, and restored later, when the gravity values for validation purposes are synthesized. With the regional gravity modeling approach, only a residual gravity signal is represented. Three different sets of validation data defined on the topography are provided, one in a larger area and two in a smaller area. We use the one which fits best with the area of observations for the different types of observations.

**Table 1** Summary of the modeling results

<i>Individual data sets</i>				
Type of observations	Error RMS%	$N$ kernel	Margin width [°]	
GRACE-type	2.1	300	0	
GOCE-type	1.26	350	0	
Terrestrial, 30' spacing	1.55	300	0	
Terrestrial, 5' spacing	0.21	1,200	2	
Aerial, case I	0.40	700	1	
Aerial, case II	0.37	900	1	
<i>Combination of the data sets</i>				
Type of observations	Error RMS% appr. A	Error RMS% appr. B	$N$ kernel	Margin width [°]
GRACE + terrestrial (30')	1.28	0.95	350	0
GRACE + GOCE	2.26	1.26	350	0
Aerial case I + terrestrial (5')	0.35	0.22	1,200	2
GRACE + aerial case I + aerial case II	2.3	2.7	350	2
GRACE + aerial case I + terrestrial (5')	0.65	0.17	1,000	2

**Fig. 1** GRACE observations with white noise with a standard deviation of  $0.0008 \text{ m}^2/\text{s}^2$ , together with validation area (red box)

The modeling results, in terms of RMS error after validation, for all data sets are given in the first part of Table 1. In the following, two examples are presented in more detail. The first example are GRACE-type observations. The observations, potential differences along real GRACE orbits, are given in Fig. 1. Figure 2 shows the modeling results from the GRACE observations in terms of disturbing potential on the topography on the left hand side. The plot in the center shows the validation field, and the plot on the right hand side the difference between the two previous ones, that is, the modeling errors. The second example are aerial observations for one flight campaign. Again, Fig. 3 shows the observations and Fig. 4 the modeling results.

#### 4 Combination of the Different Data Sets

Investigations in combining heterogenous data sets have already been made, as for example in Panet et al. (2012) with a wavelet approach. We combine different data sets by determining a relative weighting, favourably related to the accuracies of the individual observation sets. For that purpose we use here the method of variance component estimation (VCE) as already mentioned before. To establish our linear model we first transform the observation equation as defined in Eq. (1) into the matrix equation  $\Delta\mathbf{F}_i + \mathbf{e}_i = \mathbf{A}_i \mathbf{d}$  where  $i = 1, \dots, n$  means an individual observation set. Then we combine the  $n$  single models to the combined model

$$\begin{bmatrix} \Delta\mathbf{F}_1 \\ \Delta\mathbf{F}_2 \\ \vdots \\ \Delta\mathbf{F}_n \\ \boldsymbol{\mu} \end{bmatrix} + \begin{bmatrix} \mathbf{e}_1 \\ \mathbf{e}_2 \\ \vdots \\ \mathbf{e}_n \\ \mathbf{e}_\mu \end{bmatrix} = \begin{bmatrix} \mathbf{A}_1 \\ \mathbf{A}_2 \\ \vdots \\ \mathbf{A}_n \\ \mathbf{I} \end{bmatrix} \mathbf{d},$$

$$D\left(\begin{bmatrix} \Delta\mathbf{F}_1 \\ \vdots \\ \Delta\mathbf{F}_n \\ \boldsymbol{\mu} \end{bmatrix}\right) = \begin{bmatrix} \sigma_1^2 \mathbf{I}_1 & 0 & \dots & 0 \\ 0 & \ddots & & \vdots \\ \vdots & & \sigma_n^2 \mathbf{I}_n & 0 \\ 0 & \dots & 0 & \sigma_\mu^2 \mathbf{I}_\mu \end{bmatrix} \quad (4)$$

which means a *Gauss-Markov model* with unknown coefficient vector  $\mathbf{d}$  and unknown variance components  $\sigma_i^2$  with  $i = 1, \dots, n$  for the  $n$  observation sets and  $\sigma_\mu^2$  for the prior

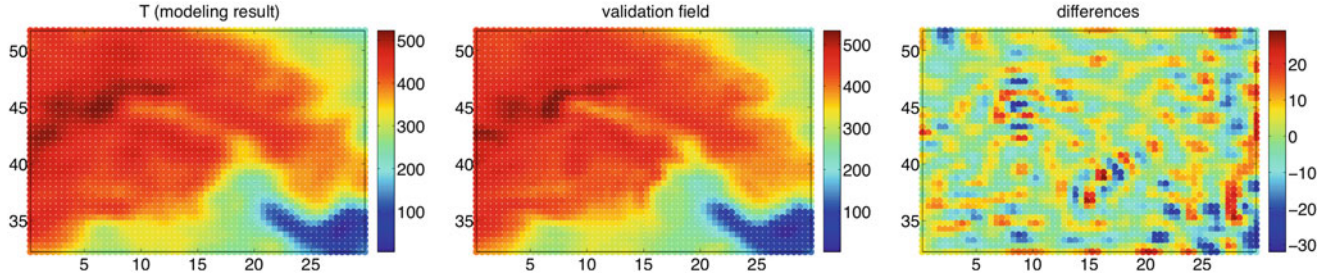


**Fig. 2** GRACE regional modeling results for a region in Europe; all results given in disturbing potential [ $\text{m}^2/\text{s}^2$ ]; relative error RMS: 2.1%

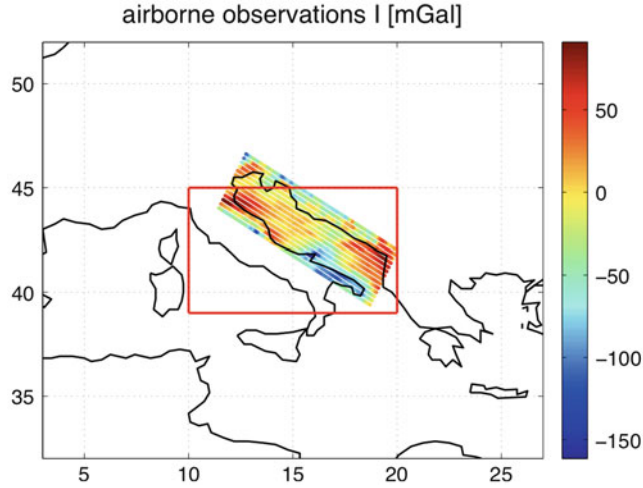


**Fig. 3** Airborne observations (case I) with white noise with a standard deviation of 1 mGal together with validation area (red box)

information. In the following we distinguish between two approaches on variance component estimation (according to the Koch and Kusche (2002)):

- (a) We introduce the assumption  $\sigma_1^2 = \sigma_2^2 = \dots = \sigma_n^2 =: \sigma_0^2$  for the  $n$  variance components  $\sigma_i^2$ . Thus, in this approach we determine the estimations of  $\mathbf{d}$  as well as  $\sigma_0^2$  and  $\sigma_\mu^2$ . The iteratively determined variance components lead—in the point of convergence—to the solution

$$\hat{\mathbf{d}} = \left( \frac{1}{\hat{\sigma}_0^2} \sum_{i=1}^n \mathbf{A}_i^T \mathbf{A}_i + \frac{1}{\hat{\sigma}_\mu^2} \mathbf{I}_\mu \right)^{-1} \left( \frac{1}{\hat{\sigma}_0^2} \sum_{i=1}^n \mathbf{A}_i^T \Delta \mathbf{F}_i + \frac{1}{\hat{\sigma}_\mu^2} \mathbf{I}_\mu \boldsymbol{\mu} \right)$$

for the unknown coefficient vector  $\mathbf{d}$ .

- (b) Besides the unknown coefficient vector  $\mathbf{d}$  we here introduce all  $n + 1$  variance components  $\sigma_i^2$  for  $i = 1, \dots, n$  and  $\sigma_\mu^2$  defined in the model (4) as unknown parameters. With the estimation of the individual variance components the relative weighting between all observation sets and the prior information is determined. Thus, the VCE yields in the point of convergence the solution

$$\hat{\mathbf{d}} = \left( \sum_{i=1}^n \frac{1}{\hat{\sigma}_i^2} \mathbf{A}_i^T \mathbf{A}_i + \frac{1}{\hat{\sigma}_\mu^2} \mathbf{I}_\mu \right)^{-1} \left( \sum_{i=1}^n \frac{1}{\hat{\sigma}_i^2} \mathbf{A}_i^T \Delta \mathbf{F}_i + \frac{1}{\hat{\sigma}_\mu^2} \mathbf{I}_\mu \boldsymbol{\mu} \right).$$

The different sets of observations are combined according to the two approaches discussed before. The modeling results from these two combinations are presented in the lower part of Table 1. In Fig. 5 the modeling results for one combination example are presented.

## 5 Regional Modeling Results

In Table 1, all modeling results from the ICCT study group test data for the region in Europe are summarized. For each set of observations, the relative RMS error is given in %-values together with the maximum degree in the cubic polynomial basis function and a margin width which is used in order to avoid boundary effects. The values given in [°] indicate by how much the validation area is smaller than the area of observations. For the results obtained from combination of different data sets the error RMS% values are given for both of the approaches outlined before. The results from satellite based observations lead to slightly worse results than the other observations. This is due to the downward continuation problem of gravity, which is of course included when gravity on the Earth surface is computed from observations at satellite orbit height. Downward continuation is an ill-posed problem by its physical nature, the gravity signal gets attenuated with distance from the masses. The terrestrial observations with 30' spacing lead as well to an RMS error which is not as low as from the other terrestrial data sets. This is due to the fact that also in the observations with 30' spacing, information up to spherical harmonic degree 2,190 was included. But the spacing of observations is not dense enough to sample this high frequency signal. Thus, not the full signal content can be recovered from the coarse observations. The very dense sampling of the terrestrial observations with 5' spacing as well as from the aerial observations lead



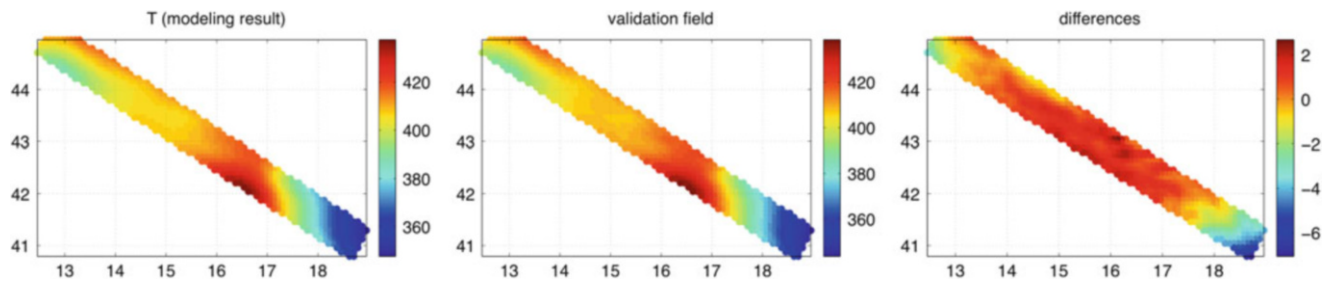


**Fig. 4** Regional modeling results for a region in Europe, from aerial observations, case I. All fields are disturbing potential, in  $[m^2/s^2]$ ; relative error RMS: 0.40%

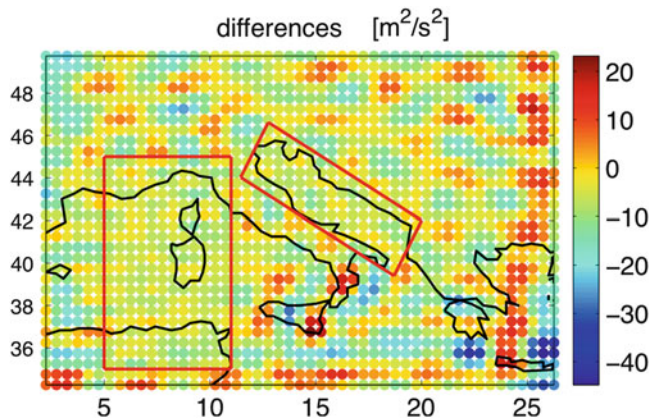


**Fig. 5** Regional modeling results for a simultaneous analysis of GRACE and two sets of aerial observations. The plot shows the difference in the disturbing potential field on the topography synthesized from the modeling approach and the reference field. That is, the modelling errors in  $[m^2/s^2]$ . The *red boxes* indicate the area of the two flight campaigns (called case I and II). GRACE observations (see Fig. 1) are available throughout the whole area. The relative error RMS is 2.3% and the plot shows that the errors are small in the areas where aerial observations are available, but high outside

to very small errors in the recovered signal. The spacing of the sampling is dense enough to recover the maximum frequency in the signal (spherical harmonic degree 2,190). The terrestrial observations lead to even better results than the aerial observations, since in the terrestrial observations no downward continuation of gravity is included, while in the aerial observations it still plays a role.

In the data combination results in the second part of Table 1 approach B, with individual weights for the data sets, generally leads to better results than approach A. The only exception is the combination of GRACE data with the two sets of aerial results. This special case is discussed in the following in more detail.

In the combination of GRACE-type and terrestrial observations with  $30'$  spacing it can be seen how additional terrestrial observations lead to a better result. The combined error is lower than the individual errors. This also holds for the combination of GRACE and GOCE data, however, when

two satellite-based data sets are combined, the result does not improve that much. The combination of aerial and terrestrial observations leads to good results, since the error RMS of the aerial data can be significantly improved by adding terrestrial observations.

The results of combining GRACE-type observations and the two aerial data sets show that even if the two aerial data sets cover a reasonable part of the area of interest (but still less than half of the area), this is not enough to make the solution of the whole area significantly better than from GRACE observations alone. For validation, the data set with spherical harmonic degrees up to 2,190 was chosen. These high degrees can not be recovered in the areas where only GRACE data is available and with a basis function of only degree 350. Therefore, the overall RMS% error is even higher than for GRACE data alone. Furthermore, the results for approach B are even worse than for approach A, since in this non-realistic scenario, no appropriate variances can be assigned to the data sets, and the errors outside the areas of aerial observations get very high.

Finally, the combination of three different types of data sets, namely satellite-based, aerial and terrestrial observations, leads to very good modeling results. The error RMS value is amongst the lowest to be achieved.

## 6 Summary and Outlook

Different types of gravity observations can be combined in one parameter estimation step in the regional gravity field modeling approach in spherical radial basis functions. The different sets of observations can be directly used in the approach, without prior processing or gridding of the observed values. The results presented in this paper are not only useful for comparisons with other methods for the ICCT study group, but they are also a first step towards the analysis of real observations. All results shown above are obtained from simulated observations with a realistic noise level according to the ICCT study group. They lead to modeling errors between 0.2 and 2% for the different scenarios.

Due to more and more available high-resolution gravity observations, regional gravity modeling techniques play an important role, since the common approach of gravity modeling in spherical harmonic basis functions cannot accommodate regional gravity refinements appropriately. However, using real data in the regional modeling approach would be more tricky than this simulation, e.g. due to coloured noise of and correlations between the observations. In order to take the simulation study closer to processing real observations, stochastic properties of the different data types could be considered and improved in the variance component estimation step as well.

**Acknowledgements** This study was made possible through funding by a “DAAD Doktorandenstipendium” from the German Academic Exchange Service.

---

## References

- Bentel K, Schmidt M, Gerlach C (2013) Different radial basis functions and their applicability for regional gravity field representation on the sphere. *Int J Geomath* 4:67–96. doi:10.1007/s13137-012-0046-1
- Drinkwater MR, Haagmans R, Muzi D, Popescu A, Floberghagen R, Kern M, Fehring M (2007) The GOCE gravity mission: ESA's first core Earth explorer. In: Proceedings of 3rd international GOCE user workshop, 6–8 November, 2006, Frascati, Italy, ESA SP-627, pp 1–8
- Freedon W, Gervens T, Schreiner M (1998) Constructive approximation on the sphere with applications to geoscience. Oxford Science, Oxford. ISBN 019853682
- Holschneider M, Chambodut A, Mandea M (2003) From global to regional analysis of the magnetic field on the sphere using wavelet frames. *Phys Earth Planet Inter* 135(2–3):107–124. doi:10.1016/S0031-9201(02)00210-8
- Koch KR, Kusche J (2002) Regularization of geopotential determination from satellite data by variance components. *J Geod* 76:259–268. doi:10.1007/s00190-002-0245-x
- Panet I, Kuroishi Y, Holschneider M (2012) Flexible dataset combination and modelling by domain decomposition approaches. In: Sneeuw N, Novak P, Crespi M, Sanso F (eds) VII Hotine-Marussi Symposium on Mathematical Geodesy, International Association of Geodesy Symposia, vol 137. Springer, Berlin/Heidelberg, pp 67–73. doi:10.1007/978-3-642-22078-4\_10
- Schmidt M, Fengler M, Mayer-Gürr T, Eicker A, Kusche J, Sánchez L, Han SC (2007) Regional gravity modeling in terms of spherical base functions. *J Geod* 81(1):17–38. doi:10.1007/s00190-006-0101-5
- Tapley B, Bettadpur S, Watkins M, Reigber C (2004) The gravity recovery and climate experiment: Mission overview and early results. *Geophys Res Lett* 31:L09607. doi:10.1029/2004GL019920